

Development of corrosion protective polymeric coatings from a non-edible seed oil

Entwicklung einer Polymerbeschichtung zum Schutz vor Korrosion gegen Bioöl

M. Alam¹, M. R. Shaik², N. M. Alandis²

In this study, we have developed corrosion protective coatings material from *Pongamia glabra* seed oil. First, oil was converted to pongamia oil epoxy (POE). The resin was synthesized by the reaction of POE with phthalic acid to develop polyester (PE) and further treated with diethylene triamine (DTA) in different (20–35%wt) amount. The structural elucidation of POE and PE were carried out by FT-IR, ¹H-NMR and ¹³C-NMR spectroscopic techniques. Thermal behavior of PE-30 was studied by thermogravimetric analyses (TGA) and differential scanning calorimetry (DSC). The coatings of PE-DTA resins were prepared on mild steel strips to investigate their physico-mechanical and corrosion performance. Corrosion protection of coated panels were examined in different corrosive media (3.5 wt% HCl, 3.5 wt% NaOH, 5.0 wt% NaCl) using potentiodynamic polarization and AC impedance. Thermal analyses revealed that PE-30 may find application as eco-friendly corrosion protective coating safely used up to 175 °C.

Keywords: pongamia glabra / Precipitates / oil epoxy / coatings

Schlüsselwörter: Pongamia fladbra / Ablagerung / Edpoxidöl / Beschichtungen

1 Introduction

Polymeric materials derived from renewable natural resources have been enjoying a continuous growing interest in the past decade from the academic and industrial point of view. The advantages of these polymers are eco-friendliness, easy availability and possible biodegradability [1–4]. The development of useful biodegradable polymeric materials has encouraged scientists to use readily available renewable raw materials like carbohydrates, lignin, starch, gums, chitosan and seed oils. Out of these, seed oils like soyabean, linseed, castor, safflower, coconut, argemone, olive are the major renewable resources [5–10]. Research and development efforts are being focused on the use of non-conventional seed oils in the field of polymer coatings.

Pongamia glabra (karanja) belongs to the family Leguminaceae. It is medium sized tree with a short crooked trunk and broad crown of spreading or drooping branches. It is considered to be a native of Western Ghats in India and occurs naturally in most parts of the Indian subcontinent [11]. It can grow under a wide range of agroclimatic conditions and is a common sight

around coastal areas, riverbanks, tidal forests and roadsides [12]. The tree is valued for shade, ornamental purpose, seed oil, fodder and green manure [11]. The oil content 28–32% having good amount of unsaturation with a higher concentration of oleic acid. Pongamia seed oil (PO) is reportedly used in bio-diesel as well as in surface coatings [12–14]. In the field of surface coatings, many seed oils are used through a different route to develop various polymers like alkyd, polyepoxy, polyesteramide, polyetheramide, polyesters and others [5, 6, 15, 16].

Phthalic acid is generally used in the area of polymers for the preparation of polyesters, polyesteramides, polyurethanes and others [7, 9]. Aliphatic/aromatic amines such as diethylene triamine (DTA) is used as a curing agent for different types of polymers like epoxy, polyester, polyesteramide [7, 17–24]. It contains three amine groups in one molecule-two primary amines at the end of ethyl group and one secondary amine in between two ethyl chains. Therefore, we expect this amine as a useful good curing agent for a oil based polyester system.

In this article, we have reported the epoxidation of pongamia glabra seed oil through per acetic acid in *situ* reaction [7, 25, 26]. Epoxidised PO (POE) is further treated with PA to form polyester (PE); the latter is further cured with DTA and used as coating material for mild steel. A voluminous literature reports that acid/anhydride and amine curing agent are used for commercial epoxy resins like diglycidyl ether of bisphenol A (DGEBA) [27]. Physico-chemical characterizations such as refractive index, specific gravity, iodine value, saponification values and coating properties of the resins were carried out by standard laboratory methods. The system may be used as a potential candidate for coating applications.

¹ Research Centre-College of Science, King Saud University, Riyadh 11451, Kingdom of Saudi Arabia

² Department of Chemistry, College of Science, King Saud University, Riyadh 11451 Kingdom of Saudi Arabia

Corresponding author: Manawwer Alam, Research Centre-College of Science, P. O. Box 2455, King Saud University, Riyadh 11451, Kingdom of Saudi Arabia

E-mail: malamiitd@gmail.com

2 Materials and methods

Pongamia glabra seeds were finely powdered in a grinder. Oil was extracted from seeds powder in a Soxhlet apparatus by refluxing in petroleum ether (BP. 60–80 °C). PO was separated from the solvent in a rotary evaporator and was suitably purified. The fatty acid composition of the oil was determined using its methyl ester on a Perkin Elmer Model 716, Column: SUPLEO-WAX (0.32 id and 30 meter long), gas liquid chromatography with FID detector. The injection temperature was 260 °C; nitrogen/helium and hydrogen were used as the carrier gas at a flow rate of 300 ml/min and 30 ml/min. The fatty acid composition of PO was found as Oleic 53.10%, Linoleic 20.00% Palmitic 11.25%, Stearic 8.08%,

Mild Steel specimens (Fe = 99.51%, Mn = 0.34%, C = 0.10%, P = 0.05%), hydrogen peroxide 30% (Winlab, Wilfind Smith Ltd, Middlesex, HA8 7ET, UK), acetic acid (Polyscience, Warrington, PA), sulphuric acid, sodium hydroxide, sodium chloride, diethylene triamine, phthalic acid (PA) (BDH Chemicals, Ltd Poole, England) were used as received.

POE was characterized by FT-IR ¹H-NMR and ¹³C-NMR spectroscopic techniques. FT-IR spectrophotometer (Prestige-21, FTIR-8400S, Shimadzu Corporation, Kyoto, Japan) using NaCl cell. ¹H-NMR and ¹³C-NMR spectrum were recorded on a Jeol DPX400 MHz using deuterated chloroform (CDCl₃) as solvent and TMS as an internal standard. Thermal analysis was carried out by Q 500 (TA Instrument USA) in nitrogen atmosphere at a heating rate of 10 °C/minute. The physico-chemical properties such as iodine value (ASTM D1959-97), hydroxyl value (ASTM D1957-86), acid value ASTM D555-61, saponification value (ASTM D94) and refractive index were determined by standard laboratory methods.

Different composition of PE-DTA coatings were prepared by brush technique using 40 wt% of the resin in solvent (butanone) on commercially available mild steel (MS) strips of 30 × 10 × 1 mm for chemical resistance and 70 × 25 × 1 mm for gloss, scratch hardness (BS 3900), impact resistance (IS; 101 part 5/sec-3, 1998) and bend test (ASTM-D 3281-84). The MS-strips were first polished with silicone carbide papers of various grade (120, 180 up to 1200), rinsed with alcohol and acetone followed by drying with hot air, and then coated with PE-DTA solution. The coatings were dried at room temperature.

The specular gloss was determined at 45° by Glossmeter, Model, RSPT 20, (Digital Instrument, Santa Barbara). Coating thickness was measured by Elcometer Model 345 (Elcometer Instruments, Manchester, UK). Thickness of these coatings was found between 70–100 μm. The films become dry-to-touch within 25 minutes and complete curing reaction of film occurred within 8 days. All physico-mechanical and corrosion resistance tests were performed after completely drying the coatings.

Electrochemical measurements were performed using a conventional three electrodes system at room temperature, a platinum electrode as counter electrode, saturated calomel electrode (SCE) as reference electrode and MS specimen as working electrode (anode). The Specimen was embedded by Polytetrafluorethene (PETE), exposed to a surface area of 1.0 cm² to different corrosive aqueous media e.g. HCl (3.5 wt%), NaOH (3.5 wt%) and NaCl (5 wt%) solution. The Tafel polarization curve was

obtained using a scan rate of 1 mV/s in the potential range of ±250 mV. Electrochemical Impedance Spectroscopy (EIS), was used to measure the resistance of the coating. EIS is based on the measurement of the current response on small sinusoidal perturbation of the electrode potential as a function of the frequency [28]. EIS were obtained at the frequency range of 0.01 Hz to 10000 Hz with amplitude of 5 mV/s. Potentiodynamic (Tafel) polarization and Nyquist impedance curve were plotted using a computer controlled Auto ACDSP (ACM Instruments) with Boukmap software.

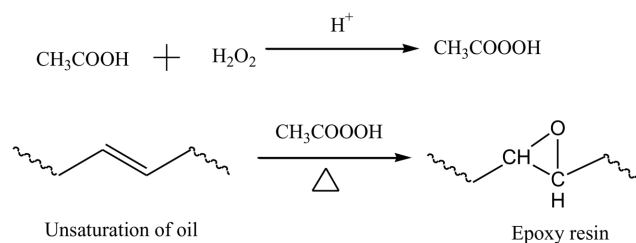
The linear Tafel segments of the anodic and cathodic curves were extrapolated to corrosion potential to obtain the current densities (*I*_{corr}). Inhibition Efficiency (*IE*) values were calculated from the *I*_{corr} values following equation [29].

$$IE(\%) = \frac{I_{corr}^0 - I_{corr}}{I_{corr}^0} \times 100$$

Where *I*_{corr}⁰ and *I*_{corr} are the corrosion current density of bare and coated MS in different corrosive media respectively

2.1 Synthesis of pongamia oil epoxy (POE)

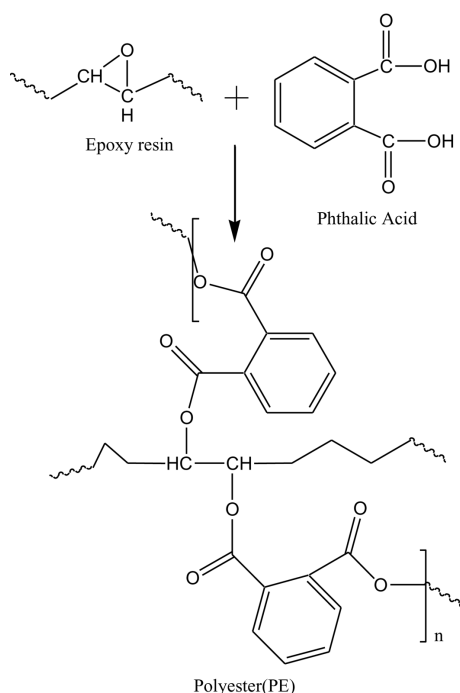
POE was prepared according to a previously reported method [7, 8]. Pongamia oil 40 ml, 40 ml benzene, 8.0 ml glacial acetic acid and 1 ml of sulphuric acid diluted to 50% with deionized water were taken in a three-necked round bottom flask equipped with a mechanical stirrer, dropping funnel and thermometer. The flask was immersed in cold water bath; 48.5 ml of 30% hydrogen peroxide was added drop wise with continuous stirring. The temperature of the reaction mixture was kept at 0–5 °C during the addition of hydrogen peroxide, then raised up to 60 °C. The progress of the reaction was monitored by determining the epoxy equivalent (EE) at regular intervals. When EE approached 350, the reaction was stopped. The synthesized POE was cooled and dissolved in diethyl ether and washed with 15% NaCl aqueous solution and separated in two layers, then the aqueous layer was discarded and the ethereal layer was taken in a round bottom flask. Ether was removed with the help of rotary vacuum evaporator and finally yellow viscous POE was obtained (Scheme 1).



Scheme 1. Synthesis of Pongamia oil epoxy(POE)

2.2 Preparation of coating material

POE (8.30 gm, approx 0.01 mol) and phthalic acid (4.02 gm, 0.03 mol) were taken in a three necked round bottom flask fitted with a nitrogen inlet tube, a condenser, a thermometer and a magnetic stirrer. The temperature of the reaction was maintained at 140 ± 5 °C. The progress of the reaction was monitored by thin layer chromatography and epoxy equivalent (EE) at regular inter-



Scheme 2. Synthesis of Polyester(PE)

vals of time. When the reaction was completed, the excess solvent was removed from PE in rotary vacuum evaporator (Scheme 2).

DTA was added in different (20–35) wt% in the above product and also ethyl methyl ketone as solvent at 50±5 °C to obtain a series of PE-20, PE-25, PE-30, PE-35.

3 Results and discussion

The formation of POE and PE were further confirmed by FTIR, ^1H NMR and ^{13}C NMR spectral analyses.

3.1 Spectral analysis of POE [7, 8]

FTIR cm^{-1} 3004 (C–H stretching of unsaturation); 2924 (–CH₂–, –CH₃, asymmetric str), 2852 (–CH₂–, –CH₃, asymmetric str); 1743 (C=O ester); 1626 (HC=CH stretching); 1242, 1165 and 1107 (C–C(=O) str and –O–C–C str of ester); 920–845 (oxirane).

^1H -NMR (CDCl_3): 5.22 (CH=CH) 4.25–4.11 (–CH₂, glycerol); 2.86 (–CH oxirane); 1.57–1.22 (–CH₂ fatty acid chain); 0.85–0.82 (–CH₃ fatty acid chain), Fig. 1.

^{13}C -NMR (CDCl_3): 173.29 (C=O); 126.02 (CH=CH); 68.95–62.12 (–CH₂, glycerol); 54.38–54.22 (C, oxirane); 29.73–26.63 (–CH₂ fatty acid chain); 14.13 (CH₃), Fig. 2.

3.2 Spectral analysis of PE

FTIR cm^{-1} 3004 (C–H stretching of unsaturation); 2924 (–CH₂–, –CH₃, asymmetric str), 2853 (–CH₂–, –CH₃, asymmetric str); 1742 (C=O ester); 1601 (HC=CH stretching); 1257, 1165 and 1070 (C–C(=O) str and –O–C–C str of ester); 3050, 1600, 742 (aromatic ring).

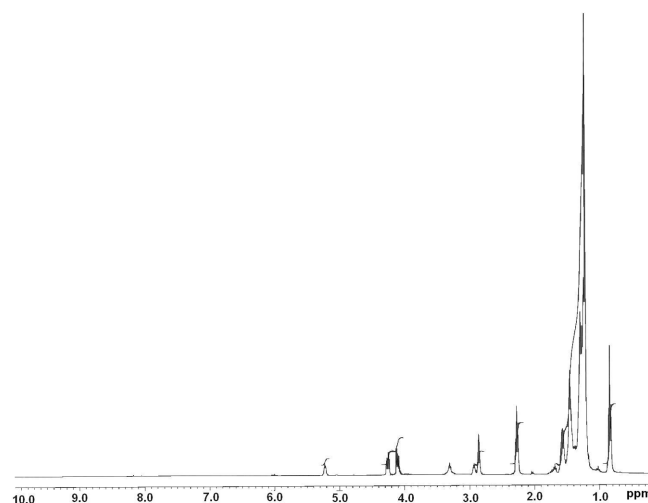


Fig. 1. ^1H -NMR spectra of POE

^1H -NMR (CDCl_3): 5.23 (CH=CH) 4.26–4.11 (–CH₂, glycerol); 7.54–7.52 (aromatic ring); 1.57–1.22 (–CH₂ fatty acid chain); 0.84–0.82 (–CH₃ fatty acid chain), Fig. 3.

^{13}C -NMR (CDCl_3): 173.34 (C=O, ester); 125.72 (CH=CH); 68.95–62.14 (–CH₂, glycerol); 130.04–129.61 (aromatic ring); 29.77–22.75 (–CH₂ fatty acid chain); 14.19 (CH₃), Fig. 4.

3.3 Physico-chemical analysis

Physico-chemical characterizations values are provided in Table 1. The decreasing trend in iodine, saponification, hydroxyl values from PE and subsequently to PE-20, PE-25, PE-30, PE-35 is observed. The increase in refractive index and inherent viscosity from PE to PE-20, PE-25, PE-30, PE-35 after addition of DTA can be attributed to the increase in molar mass of the resin.

3.4 Physico-mechanical properties of coatings

The PE-DTA resins were applied on mild steel strips of standard size to evaluate their coating properties. It was found that PE-20, PE-25, PE-30 and PE-35 take 30–40 minutes to become dry-to-touch. Further increase in the amount of DTA in resin causes gelation within six hours. It was found that the optimum cross-linking required to attain the dry to touch stage is achieved in PE-30.

An examination of Table-1 reveals that the scratch hardness, impact resistance and bend test values of PE-20, PE25, PE30 and PE-35 increase with the increasing the DTA. The enhancement in these properties may be correlated to increased polar groups of PE and C–N linkages, which provides sufficient adhesion and toughness to the coatings. All composition of PE-DTA show outstanding flexibility and impact resistance (1/8 inch conical mandrel bend test and 150 lb/inch) conferred by ester linkages and the fatty amide chains. The gloss at 45° was found to be between 50–59. It appears that adhesion and stiffness of the PE-25 coatings is best which endows it with the best physico-mechanical properties.

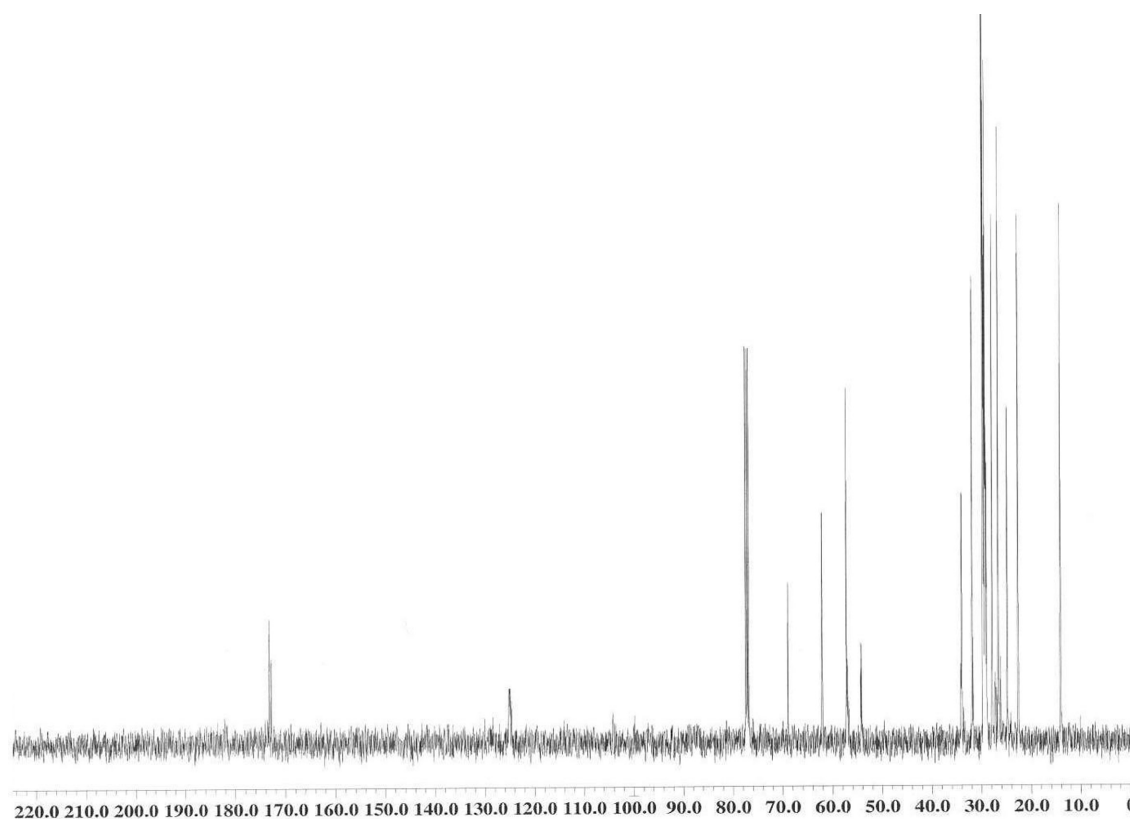


Fig. 2. ^{13}C -NMR spectra of POE

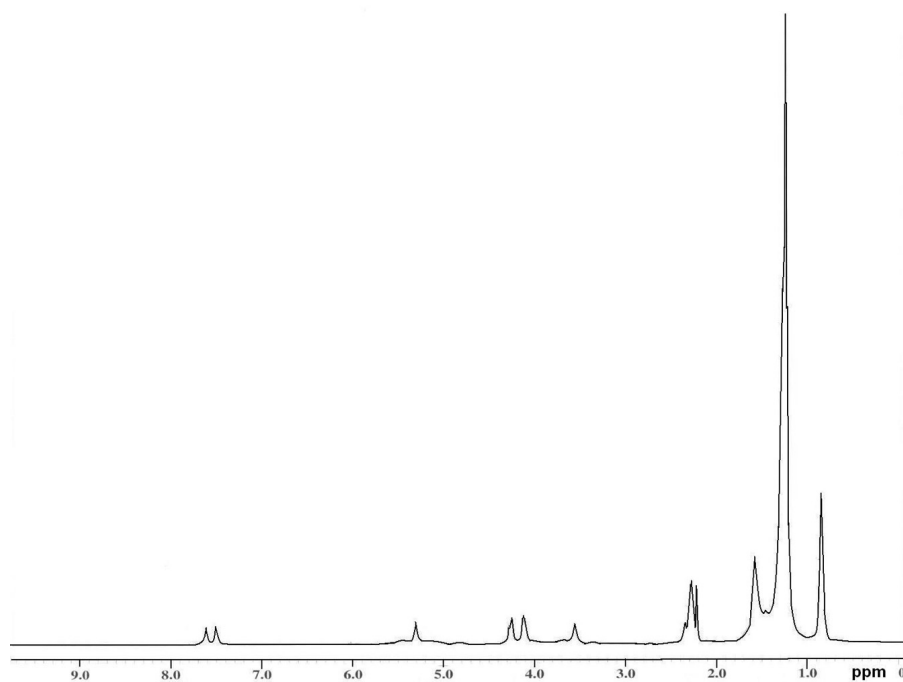


Fig. 3. ^1H -NMR spectra of PE

3.5 Potentiodynamic polarization studies

Fig. 5 shows potentiodynamic polarization curves for MS in 3.5 wt% NaOH with and without coatings. It was obvious that the polarization curves for coated MS showed a remarkable

potential shift to noble values compared to bare MS. The various parameters such as corrosion potential (E_{corr}) and current density (I_{corr}) obtained from cathodic and anodic curve by extrapolation of Tafel line are given in Table 2. It should be mentioned that

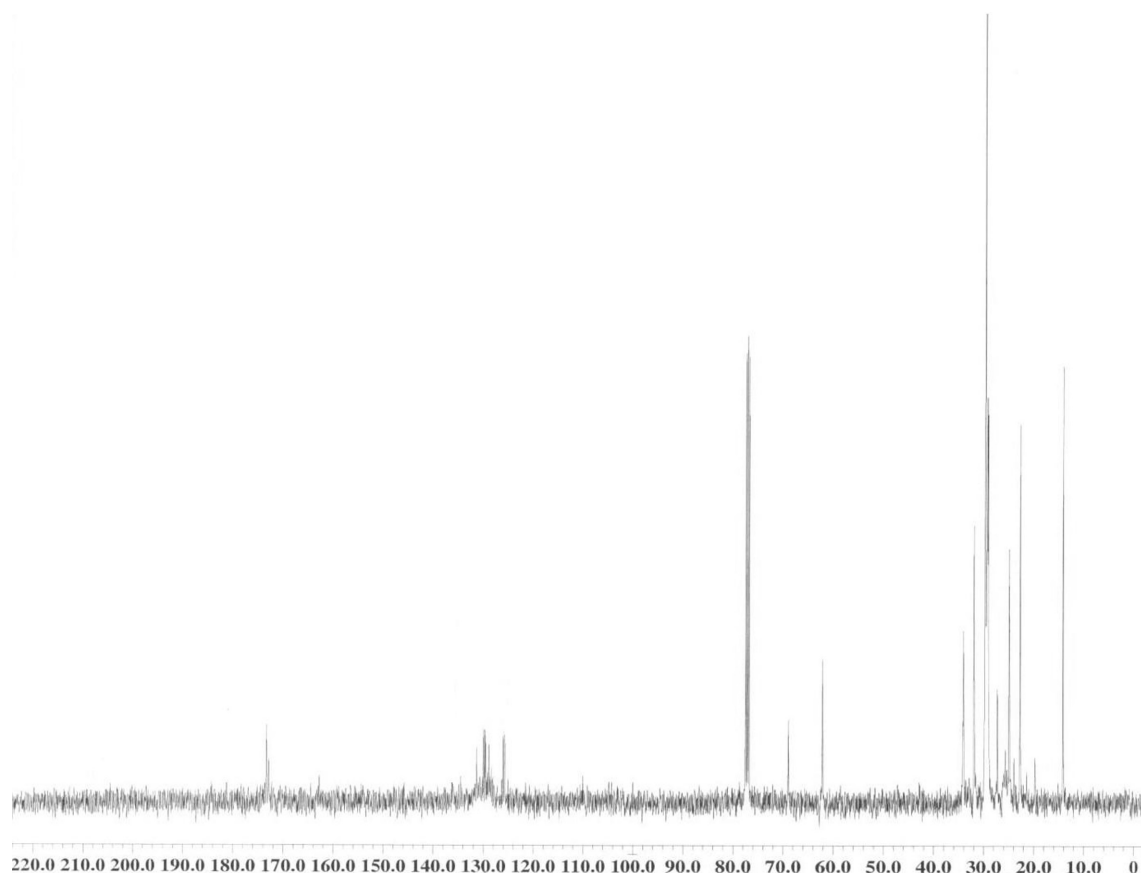
Fig. 4. ^{13}C -NMR spectra of PE

Table 1. Physico-chemical and physico-mechanical characterization of PE resins

Resin code*	PO	POE	PE	PE-20	PE-25	PE-30	PE-35
Hydroxyl value	0.16	0.12	1.20	0.13	0.11	0.10	0.91
Iodine value	85.80	12.09	10.05	8.07	7.57	7.01	6.54
Acid value	4.99	5.17	12.40	11.01	10.53	8.78	8.06
Saponification value	151.00	109.01	120.01	85.04	83.17	82.51	81.68
Refractive index	1.485	1.493	1.577	1.575	1.570	1.568	1.563
Inherent viscosity	–	0.8656	0.8908	0.9123	0.9306	0.9397	0.9403
Gloss at 45°	–	–	–	50	53	59	55
Scratch hardness(kg)	–	–	–	1.2	1.35	1.5	1.5
Impact resistance (lb/in)	–	–	–	150	150	150	150
Bending (1/8 in)	–	–	–	Passes	Passes	Passes	Passes

* Last numeral digit of resin code indicate the loading of amine

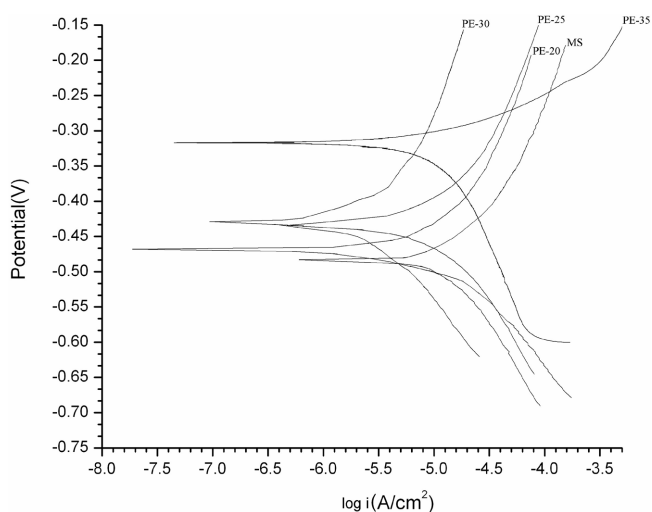
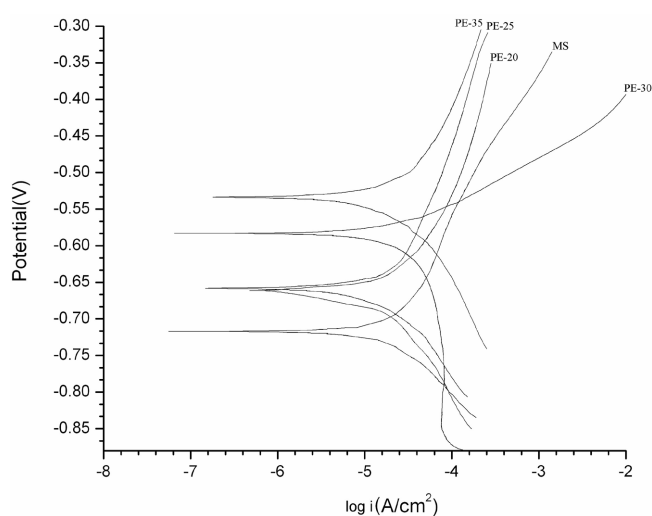
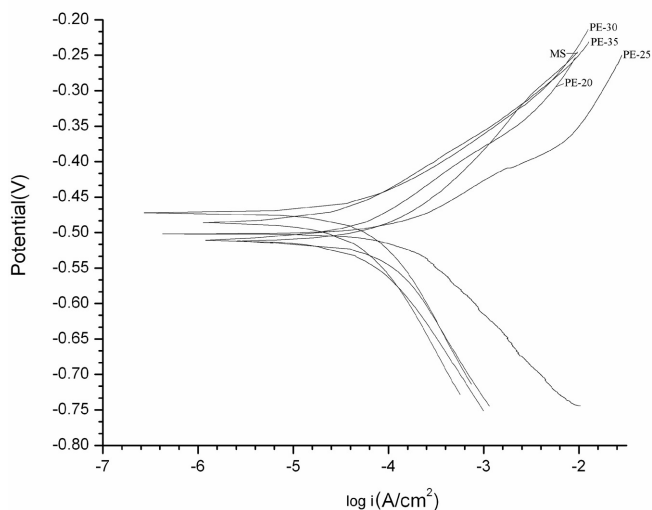
the values increased significantly for MS with coatings PE-20, PE-25, PE-30 and PE-35. This observation clearly showed that coated MS controls both cathodic and anodic reactions and thus coatings act like inhibitors. In case of MS coated with PE-20, PE-25, PE-30 and PE-35 the values were found to increase with the amount of DTA and these values -0.466 , -0.433 , -0.428 and -0.316 V respectively. On the other hand the I_{corr} values were found to decrease with an increase in the amount of DTA in PE-20, PE-25, PE-30 and PE-35. This behavior was attributed to a poor adhesive effect of PE-20 than PE-35. The corrosion rates calculated for coated MS are given in Table 2. The coated MS

showed significantly better resistances than bare MS. For instance, the corrosion rate for bare metal was found to be 5.391 mm/yr and is minimized by the application of coatings PE-20, PE-25, PE-30 and PE-35 to a lower values of 1.002×10^{-3} mm/yr, respectively. Therefore it was suggested that the examined coating on MS restricts the interaction between the metal and NaOH solution.

Fig. 6 shows the Tafel plots of uncoated MS, coated PE-20, PE-25, PE-30 and PE-35 in 3.5 wt% HCl. E_{corr} (-0.514 V vs SCE for MS) showed a positive shift for the coated samples. It was observed that the value of E_{corr} for PE-35 was higher than PE-

Table 2. Electrochemical parameters for coated and uncoated mild steel strips in different corrosive environments

Sample code	Medium	E_{corr} (V)	I_{corr} (A/cm ²)	Corrosion rate (mm/year)	Inhibition efficiency (%)
MS	3.5 wt% NaOH	-0.487	8.878×10^{-4}	5.391	–
PE-20	3.5 wt% NaOH	-0.466	5.669×10^{-4}	2.716×10^{-2}	36.145
PE-25	3.5 wt% NaOH	-0.433	4.663×10^{-4}	1.844×10^{-3}	47.476
PE-30	3.5 wt% NaOH	-0.428	2.349×10^{-4}	1.026×10^{-3}	73.541
PE-35	3.5 wt% NaOH	-0.316	1.595×10^{-4}	1.002×10^{-3}	82.034
MS	3.5 wt% HCl	-0.514	8.551×10^{-4}	9.885	–
PE-20	3.5 wt% HCl	-0.510	5.288×10^{-4}	8.581×10^{-2}	38.159
PE-25	3.5 wt% HCl	-0.502	4.154×10^{-5}	7.114×10^{-3}	51.420
PE-30	3.5 wt% HCl	-0.483	2.534×10^{-5}	6.398×10^{-3}	70.366
PE-35	3.5 wt% HCl	-0.472	1.905×10^{-5}	2.202×10^{-3}	77.721
MS	5.0 wt% NaCl	-0.714	8.411×10^{-5}	9.722	–
PE-20	5.0 wt% NaCl	-0.673	5.920×10^{-6}	8.453×10^{-2}	29.616
PE-25	5.0 wt% NaCl	-0.672	4.921×10^{-6}	3.556×10^{-3}	41.493
PE-30	5.0 wt% NaCl	-0.583	2.849×10^{-6}	3.294×10^{-3}	66.127
PE-35	5.0 wt% NaCl	-0.539	1.921×10^{-6}	2.221×10^{-3}	77.160

**Fig. 5.** Tafel polarization curve of PE in 3.5wt% NaOH solution**Fig. 7.** Tafel polarization curve of PE in 5wt% NaCl solution**Fig. 6.** Tafel polarization curve of PE in 3.5wt% HCl solution

20. The values of I_{corr} decrease from bare MS to PE-20, PE-25, PE-30, PE-35 respectively. The corrosion rate for uncoated MS was found to be higher than the PE-20, PE-25, PE-30, PE-35 coated samples subsequently. IE was also found to be higher in PE-20, PE-25, PE-30, PE-35 subsequently than uncoated MS. As a result of higher values of E_{corr} and lower values of I_{corr} lower corrosion rates confirms. Further the IE of the PE-35 was found to be maximum in said environment as compared to PE-20, PE-25, PE-30. But the physico-mechanical tests showed PE-30, to be best.

Fig. 7 shows the polarization curve recorded for bare MS and coated MS in 5wt% NaCl solution. The Tafel region of cathodic and anodic polarization curves are extrapolated and analyzed for quantifying the corrosion rate behavior of polymeric coating. Table 2 shows that the values of E_{corr} and I_{corr} are far lower than corresponding values for bare MS indicating the corrosion resistant feature of coatings. Potentiodynamic studies showed that the extent of IE by PE coatings to MS substrate depended on the load-

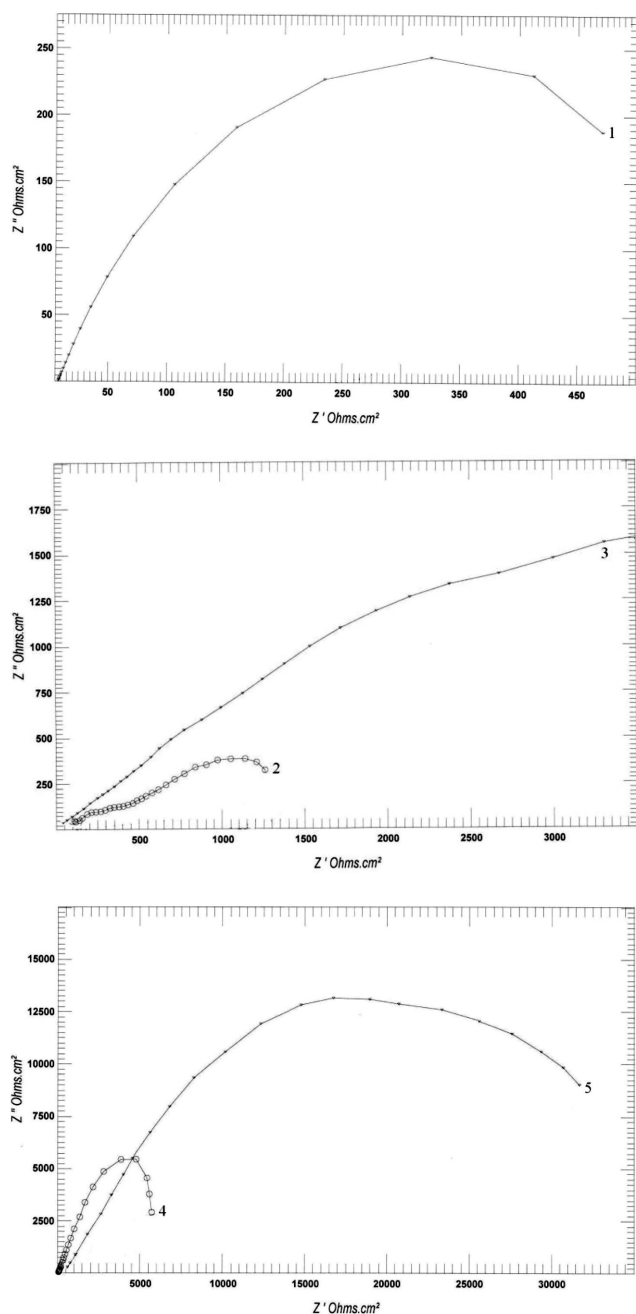


Fig. 8. Nyquist plots of PE in 5 wt% NaCl solution: (1) bare MS; (2) PE-20; (3) PE-25; (4) PE-30; (5) PE-35

ing of DTA, when increases the loading of DTA with protective performance of the coatings increases due to crosslinking density of polymer and adhesion also increases between substrate and coating, which make the coatings impermeable to the corrosive ions. Therefore PE-35 exhibits the best corrosion resistance performance among all the composition in all corrosive media show the lowest corrosion rate and maximum IE.

3.6 Electrochemical impedance studies

Fig. 8 and 9 show a Nyquist plots recorded for uncoated and coated specimens in 5 wt% NaCl, 3.5 wt% NaOH solutions

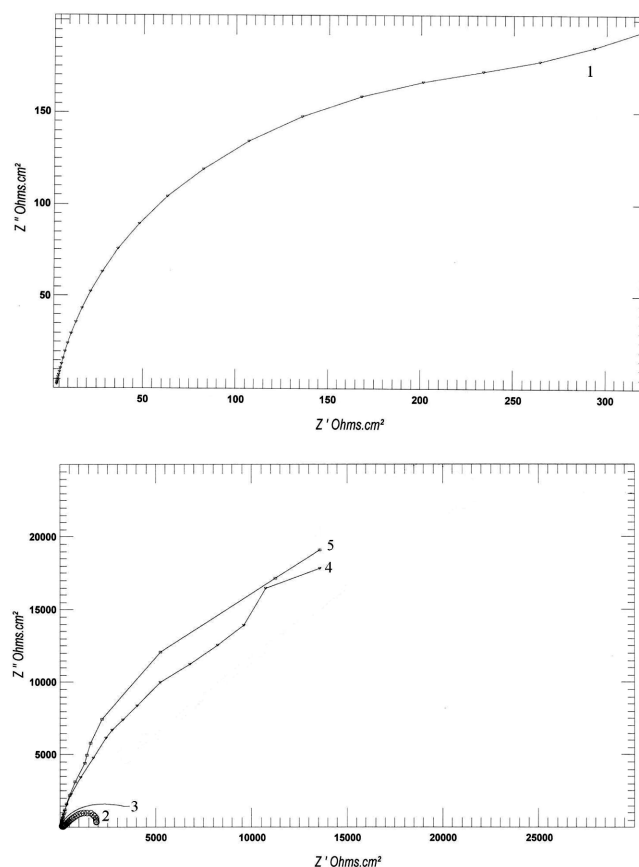


Fig. 9. Nyquist plots of PE in 3.5 wt% NaOH solution: (1) bare MS; (2) PE-20; (3) PE-25; (4) PE-30; (5) PE-35

which were using EIS at room temperature. It was apparent from these plots that the impedance response of MS has significantly changed with MS coated with PE-20, PE-25, PE-30 and PE-35. However, the Nyquist spectra for uncoated MS consisted of a depressed semicircle, which represent the interfacial (corrosion) of the system, viz., Fig. 10, the charge transfer resistance due to metal corrosion and double layer capacitance of the solution/metal interface. The deviation from the depressed semicircle in the Nyquist plots was probably due to surface heterogeneity [30]. It can be noted that the presence of a depressed semicircle and inductive loop are caused by surface homogeneity on account of active sites and the surface relaxation phenomena, respectively. Moreover, the specimen undergo a multiple redox process with more than one time constant leading to the centering of the semicircles below the real axis. This behavior is due to the charge transfer resistance related to MS dissolution and ion diffusion [30].

Fig. 11 shows the Nyquist plot in 3.5 wt% HCl solution. The Nyquist plot is composed of a semicircle followed by a diffusion tail in the lower frequency range. The semicircle in the high frequency range related to a charge transfer reaction is shown. This semicircle is due to the reductive dissolution of MS. The plot consists of an incomplete semicircle with a diffusion tail, which indicate that both electron transfer and diffusion process control the dissolution of coatings. The effect of potential on the reductive

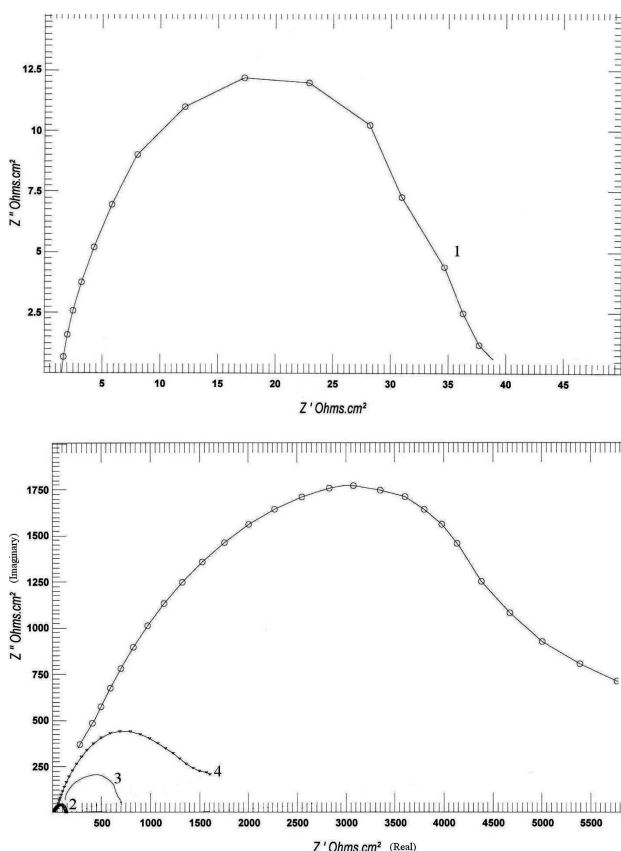
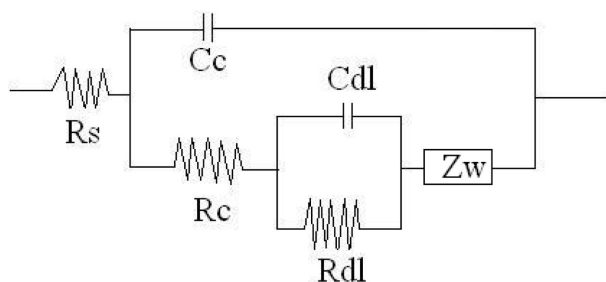


Fig. 10. Nyquist plots of PE in 3.5 wt% HCl solution: (1) bare MS; (2) PE-20; (3) PE-25; (4) PE-30; (5) PE-35



R_s → solution resistance; R_c → electric resistance of protective coating; C_c → capacitance of the protective coating; C_{dl} → double layer capacitance; R_{dl} → charge transfer resistance of the corrosive process; Z_w → Warburg finite diffusion impedance

Fig. 11. Equivalent circuit for interpreting impedance data

dissolution was interpreted by fitting the spectrum using the equivalent circuit [29] shown in Fig. 10. According to this equivalent circuit, the low frequency arc in the Nyquist diagram is related to the double layer capacitance and charge transfer at the pore base of the coating system and/or with ion transport process occurring within the pores [28]. It is clear that the charge transfer resistance of mild steel in uncoated has significantly changed after coating the panel.

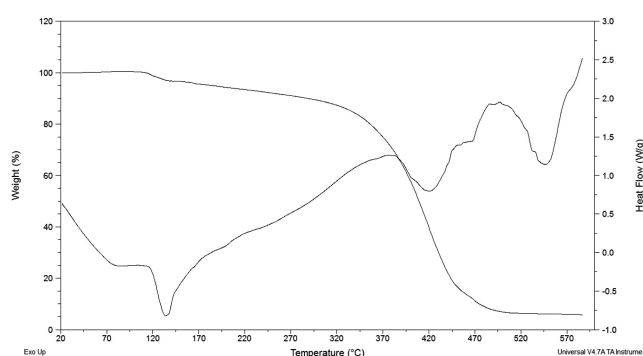


Fig. 12. DSC-TGA thermogram of PE-30

3.7 Thermal Analysis

Fig. 12 shows the TGA thermogram of PE-30. The onset of degradation occurs at 200 °C, 10% weight loss of the resins is observed at 295 °C and 50% at 413 °C. TGA thermogram demonstrated two stage degradation pattern. First stage degradation started at 285 °C and extended up to 455 °C, ahead of which second stage degradation extended up to 575 °C.

DSC thermogram of the resins shows an endothermic peak, which extends from 120 °C to 163 °C and is centered at 133 °C. In TGA thermogram, no weight loss was measured at the above mentioned temperature. Beyond 200 °C, an exotherm ensued which extended over rest of the DSC thermogram and may be attributed to decomposition of the resin since TGA thermogram clearly shows the onset of degradation beyond this temperature.

4 Conclusion

The synthesized polyester resins cured with di ethylene tri amine were evaluated for their physico-mechanical and corrosion resistance performance. PE-30 can be utilized as corrosion protective eco-friendly coating material safely up to 175 °C. This approach highlights an alternative route for the scope of the utilization of non edible seed oil in polymeric coatings.

Acknowledgement

This project was supported by King Saud University, Deanship of Scientific Research, College of Science – Research Center. Dr. Alam is also thankful to Prof. A.M. Al-Mayouf, Department of Chemistry, KSU, Riyadh for providing the facility for the measurement of corrosion test.

5 References

- [1] V. Sharma, P.P. Kumdu, *Prog. Polym. Sci.* **2006**, 31, 983.
- [2] P. Nayak, *J.M.S.-Rev. Macromol. Chem. Phys.* **2000**, C40(1), 1.
- [3] Z.S. Petrovic, *Polymer Reviews* **2008**, 48, 109.

- [4] J. Argyropoulos, P. Popa, G. Spilman, D. Bhattacharjee, W. Koone, *J. Coat. Technol. Res.* **2009**, 6(4), 501.
- [5] M. Alam, A.R. Ray, S.M. Ashraf, *J. Appl. Polym. Sci.* **2009**, 114, 3268.
- [6] M. Alam, A.R. Ray, S.M. Ashraf, *J. Am. Oil. Chem. Soc.* **2009**, 86, 573.
- [7] S. Ahmad, F. Naqvi, E. Sharmin, K.L. Verma, *Prog. Org. Coat.* **2006**, 55, 268.
- [8] E. Sharmin, S.M. Ashraf, S. Ahmad, *Int. J. Bio. Macromol.* **2007**, 40, 407.
- [9] F. Zafar, H. Zafar, E. Sharmin, S. Ahmad, *Prog. Org. Coat.* **2010**, 69, 517.
- [10] F.S. Guner, Y. Yagci, A.T. Erciyas, *Prog. Polym. Sci.* **2006**, 31, 633.
- [11] N. Mukta, I.Y.L.N. Murthy, P. Sripal, *Ind. Crop. Prod.* **2009**, 29, 536.
- [12] L.C. Meher, S.N. Naik, L. M. Das, *J. Sci. & Ind. Res.* **2004**, 63, 913.
- [13] M. Naik, L.C. Meher, S.N. Naik, L.M. Das, *Biomass and Energy* **2008**, 32, 354.
- [14] B.K. Barnwal, M.P. Sharma, *Renewable & Sustainable Energy Rev.* **2005**, 9, 363.
- [15] M. Alam, S.M. Ashraf, S. Ahmad, *J. Polym. Res.* **2008**, 15, 343.
- [16] J.L. Scala, R.P. Wool, *Polymer* **2005**, 46, 61.
- [17] L. Bonnaud, J. P. Pascault, H. Sauterau, *Eu. Poly. J.* **2000**, 36, 1313.
- [18] J. Lopez, I. Lopez-Bueno, P. Nogueira, C. Ramirez, M.J. Abad, L. Barral, J. Cano, *Polymer* **2001**, 42, 1669.
- [19] D.K. Chattopadhyay, D.C. Webster, *Prog. Org. Coat.* **2009**, 66, 73.
- [20] P.M. Remiro, M. Cortazar, E. Calahorra, M.M. Calafel, *Polym. Degrad. Stab.* **2002**, 78, 83.
- [21] G. Merfeld, C. Molaison, R. Koeniger, A.E. Acar, S. Mordhorst, J. Suriano, P. Irwin, R.S. Warner, K. Gray, M. Smith, K. Kovaleski, G. Garrett, S. Finley, D. Meredith, M. Spicer, T. Naguy, *Prog. Org. Coat.* **2005**, 52, 98.
- [22] Z.S. Liu, S.Z. Erhan, P.D. Calvert, *J. Appl. Polym. Sci.* **2004**, 93, 356.
- [23] R.F. Storey, T.P. Hickey *J. Polym. Sci-A* **1993**, 31, 1825.
- [24] Y. Tanaka, H. Kakiuchi, *J. Polymer Sci. Part A* **1964**, 2, 3405.
- [25] E. Sharmin, S.M. Ashraf, S. Ahmad, *Eur. J. Lipid. Sci. Technol.* **2007**, 109, 134.
- [26] S. Ahmad, S.M. Ashraf, E. Sharmin, F. Zafar, A. Hasnat, *Prog. Crystal. Growth Charact.* **2002**, 45, 83.
- [27] S. Ahmad, A.P. Gupta, E. Sharmin, M. Alam, S.K. Panday, *Prog. Org. Coat.* **2005**, 54, 248.
- [28] G. Grundmeir, W. Schmidt, M. Stratmann, *Electrochimica Acta* **2000**, 45, 2515.
- [29] B. Chico, J. Simancas, J.M. Vega, N. Granizo, I. Diaz, D.D.L. Fuente, M. Morcillo, *Prog. Org. Coat.* **2008**, 61, 283.
- [30] A.P. Srikankanth, S. Nanjundan, N. Rajendran, *Prog. Org. Coat.* **2007**, 60, 320.

Received in final form: May 23th 2011

T 824